Tokyo Climate Center, Japan Meteorological Agency

TCC News

No. 5 July 2006

Contents

Summary of 2005/2006 La Niña Event

A La Niña event occurred from autumn 2005 to spring 2006. It was the first La Niña event for five and a half years. Autumn was the latest season for the timing of the development and six-month duration was the shortest among the historical La Niña events since 1949. The impacts of this La Niña event on atmospheric circulation and surface climate were clear in the tropical Pacific as seen in the past events, while they were less clear in the mid- and high-latitudes.

1. Outline and main features of the 2005/2006 La Niña event

To identify El Niño/La Niña events, the SSTs of NINO.3 region (5˚S-5˚N, 150˚E-90˚E), whose interannual variability is the largest in the equatorial Pacific, are monitored in Japan Meteorological Agency (JMA). The five-month running mean values of NINO.3 SST deviation from its sliding 30-year mean were equal or below -0.5˚C for six consecutive months from October 2005 to March 2006, as shown in Table 1. JMA stated that a La Niña event occurred from autumn 2005 to spring 2006, according to the JMA's definition of La Niña events: that is, 5-month running mean SST deviation for NINO.3 continues -0.5˚C or lower for six consecutive months or longer. It is the first La Niña event for five and a half years since the 1998-2000 La Niña event. (Figure 1)

The characteristics of this La Niña event are its started season and duration length. Typically La Niña events start between spring and summer, and get to their mature phases between autumn and winter. Among all the historical La Niña events since 1949 identified by JMA, NINO.3 SST deviation turned negative in the latest timing in this La Niña event (Figure 2a). It is also seen that its minimum peak of the 5-month running mean SST deviation, -0.8˚C, was the smallest, and its duration of six months was the shortest (Table 2). So, the extent and evolution of NINO.3 SST mentioned above indicates that the 2005/2006 La Niña event was the smallest scale event among the historical La Niña events since 1949.

On the other hand, keeping our eyes on the western equatorial Pacific, the positive SST anomalies greater than +0.8˚C prevailed continually in the west of the date line from August 2005 to January 2006 (Figure 3b). The positive anomalies in the western equatorial Pacific were remarkable during this La Niña event. Figure 2b shows the difference of SST deviations between the NINO.3 region and the western Pacific region (5˚S-5˚N, 120˚E-160˚E). It is seen that the difference started to decrease after summer 2005, which was the latest timing among the historical La Niña events, but it persisted below the average of historical ones after November 2005. Therefore, from the

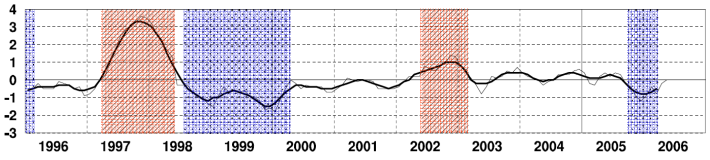

Figure 1 The time series of sea surface temperature deviation from the climatological mean based on its sliding 30-year period for NINO.3 region
Thin line indicates monthly mean values, and smoothed and thick one indicates their 5-month running mean. Red and blue shaded areas denote El Niño and La Niña periods, respectively.

Table 1 El Niño Monitoring Indices
SSTs are monthly mean sea surface temperatures averaged over NINO.3 (5˚S-5˚N, 150˚W-90˚W). The SST deviations for NINO.3 are defined as the difference between the monthly mean SSTs and the climatological means based on their sliding 30-year period. The light green shaded values in SST deviations indicate minima. 5-month mean values shaded with yellow indicate below -0.5˚C.

	2005							2006					
	Jun.	Jul.	Aug.	Sep.	Oct.	Nov.	Dec.	Jan.	Feb.	Mar.	Apr.	May	Jun.
Monthly mean SST (℃)	26.7	26.0	25.3	24.7	24.6	24.2	24.1	24.8	26.0	26.4	27.2	27.1	26.5
SST deviation (℃)	+0.2	+0.4	+0.3	-0.2	-0.4	-0.9	-1.2	-0.9	-0.4	-0.8	-0.2	0.0	0.0
5-month mean (℃)	+0.3	+0.2	+0.1	-0.2	*-0.5*	*-0.7*	*-0.8*	*-0.8*	*-0.7*	*-0.5*	-0.3	-	-
SOI	+0.4	+0.1	-0.6	+0.3	+1.2	-0.3	+0.2	+1.2	+0.1	+1.3	+1.0	-0.8	-0.4

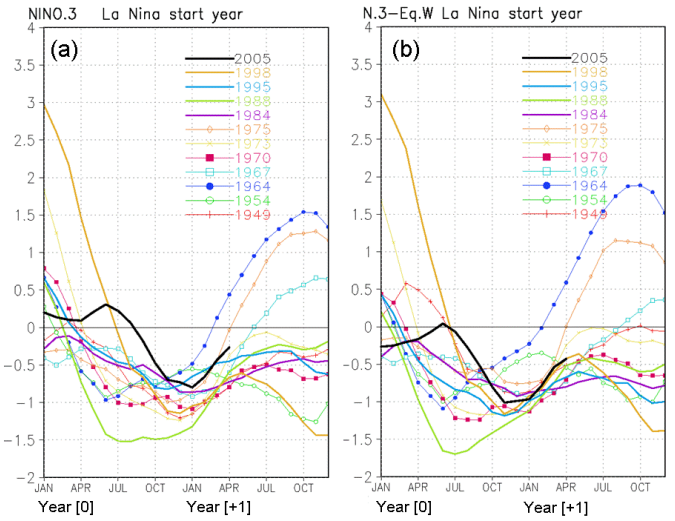

Figure 2 Time series of the 5-month running mean SST deviations (a) for NINO.3 region and (b) for NINO.3 minus the western equatorial Pacific (5°S-5°N, 120°E-160°E) in past 12 La Niña periods since 1949

Year [0] and Year [+1] indicate La Niña-occurring years and their subsequent years, respectively. Thick black lines indicate 2005/2006 La Niña. SST deviations are from their sliding 30-year mean.

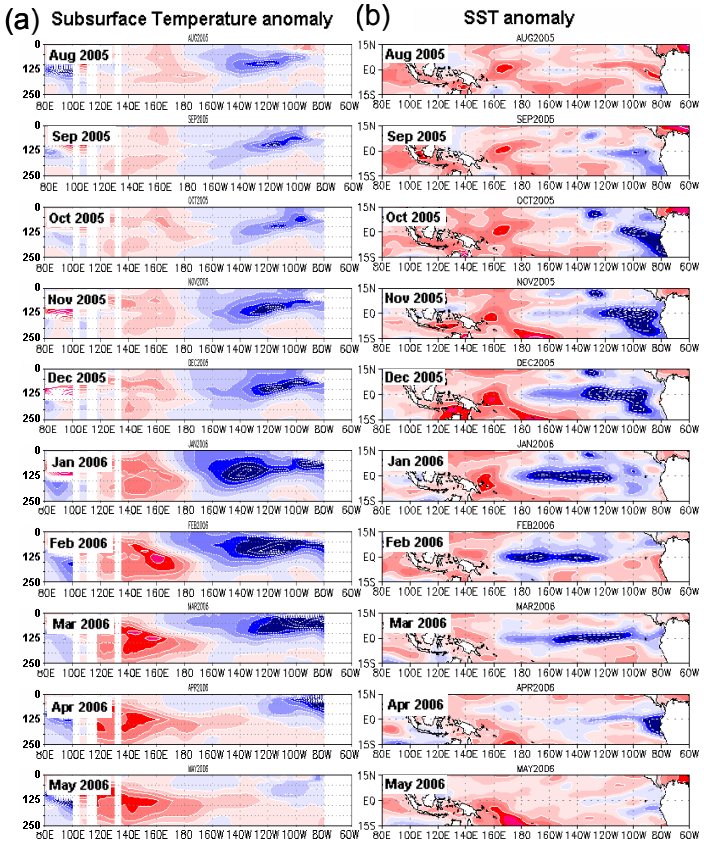

Figure 3 (a) Depth-longitude cross sections of monthly averaged subsurface temperature anomalies within upper 250 m along the equatorial Pacific and (b) Monthly averaged sea surface temperature anomalies in the equatorial Pacific

Red and blue shaded areas indicate positive and negative values, respectively. The contour intervals are 0.5°C and 0.4°C in panel (a) and (b), respectively.

Table 2 List of Historical La Niña events since 1949 based on JMA's definition

		duration		Minimum peak	
sequence number from 1949	Periods of La Niña events	The number of seasons	The number of months	5-month mean value (°C)	monthly mean value (°C)
1	Summer 1949 - Summer 1950	5	13	- 1.2	- 1.4
2	Spring 1954 - Winter 1955/56	8	23	- 1.2	- 1.7
3	Spring 1964 - Winter 1964/65	4	10	- 1	- 1.2
4	Autumn 1967 - Spring 1968	3	8	- 0.9	- 1.3
5	Spring 1970 - Winter 1971/72	8	20	- 1.1	- 1.5
6	Spring 1973 - Spring 1974	4	10	- 1.2	- 1.5
7	Spring 1975 - Spring 1976	5	12	- 1	- 1.3
8	Spring 1984 - Autumn 1985	6	15	- 0.9	- 1.1
9	Spring 1988 - Spring 1989	5	13	- 1.5	- 1.8
10	Summer 1995 - Winter 1995/96	3	8	- 0.8	- 1
11	Summer 1998 - Spring 2000	8	21	- 1.5	- 1.8
12	Autumn 2005 - Spring 2006	3	6	- 0.8	- 1.2

point of view of the east-west SST gradients, it can be said that the 2005/2006 La Niña event was above average in strength among historical La Niña events since 1949.

2. Progression of the 2005/2006 La Niña event

Figure 3 shows the evolutions of (a) monthly mean sub-surface temperature anomalies along the equator, which were analyzed using the ocean data assimilation system (ODAS) at JMA and (b) SST anomalies in the equatorial Pacific from August 2005 to May 2006.

Negative subsurface temperature anomalies were already seen in the eastern Pacific in August 2005 and the negative anomalies were strengthened and extended westward until February 2006. These negative anomalies indicate that the thermocline depths became shallower than normal there during the period.

Negative SST anomalies appeared off the South American coast in September 2005 and expanded to the central equatorial Pacific from October to December in 2005 with strengthening their negative anomaly values. In December 2005, the negative SST anomalies prevailed over NINO.3 region and monthly mean NINO.3 SST deviation from its sliding 30-year mean recorded its minimum peak of -1.2°C (Table 1). The negative SST anomalies moved westward gradually during autumn and winter, and then reached around the date line in February 2006. After that, the negative SST anomalies moved back eastward and the NINO.3 SST deviation recorded its second minimum peak of -0.8°C in March.

Under the sea surface, the positive subsurface temperature anomalies in the western Pacific were strengthened after the end of 2005, and the positive anomalies greater than +2°C have been found since February 2006. The contrast between the negative subsurface temperature anomalies in the east of date line and the positive in the west was the most remarkable during January–March in 2006. With the eastward migration of a certain amount of warm waters in the western equatorial Pacific from March to May in 2006, the negative subsurface temperature anomalies in the eastern part shrunk and SSTs became near normal over most of eastern equatorial Pacific in May 2006.

3. Impacts on the atmospheric circulation and world climate

During the 2005/2006 La Niña event, tropical convective activities across the tropical Pacific, like the past La Niña events, featured above normal over the maritime continent, the South China Sea and the western Pacific,

while below normal over the central and eastern Pacific. Consistent with the distribution of anomalous convection, the Walker circulation was stronger than normal. These features persisted from November 2005 to April 2006. However, the indices representing convective activities associated with ENSO events and the Walker circulation were not considerably large compared to the past events. As an example of these indices, Figure 4 shows time series of SOI for the past La Niña events including this event.

MJO was not prevailing during this event except from January to February. Consequently, the persistent response in the tropics associated with ENSO was more predominant than the intra-seasonal fluctuation associated with MJO.

Figure 5a (b) shows 3-month mean 200-hPa (850-hPa) stream function anomaly and outgoing long-wave radiation (OLR) anomaly in boreal winter (December 2005 to February 2006), which was the mature phase of the event.

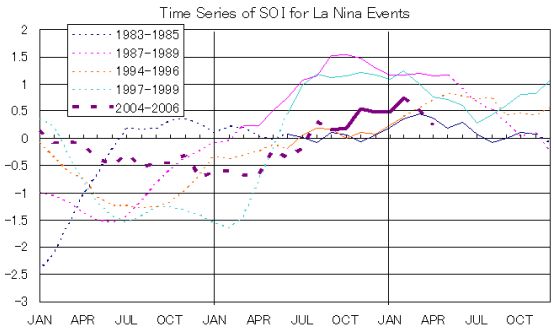

Figure 4 Time Series of SOI for La Nina Events
Three sequential years centered in the mature year are depicted. Thick violet line shows 2005/2006 La Nina event, and thin lines show five-month running mean for the past four La Nina events. The solid lines show the periods of La Nina events.

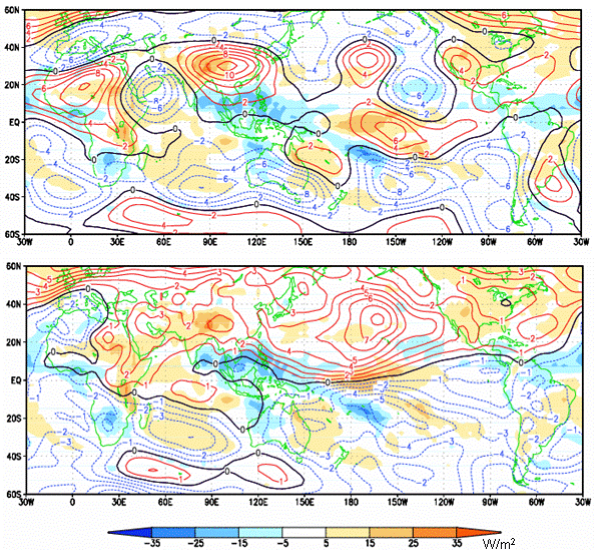

Figure 5 3-month Mean 200-hPa (upper panel)/850-hPa (lower panel) stream function anomaly and Outgoing Long-wave Radiation (OLR) anomaly (December 2005 to February 2006)
Contour in the upper (lower) panel shows stream function anomaly in an interval of 2×10^6 m^2/s (1×10^6 m^2/s). Shading in both figures shows OLR anomaly in an interval of $10 W/m^2$.

Figure 6a (b) shows 3-month mean 200-hPa (850-hPa) stream function regressed on a high cloud amount index in the vicinity of the Indonesia (5N-5S, 110E-135E), representing the typical features in general in La Niña events. The index shows the area-averaged high-cloud amount (the percentage of cloud cover whose top is above 400-hPa) anomalies normalized by its standard deviation in 1987-2000. Comparing Figure 5 with Figure 6, it can be said that the main circulation anomalies in this winter are similar to those typically observed in La Niña events, such as follows. In the upper troposphere (200-hPa), equatorial-symmetric cyclonic anomalies were dominant in the eastern Pacific, while anti-cyclonic anomalies were dominant across eastern Asia, Australia to southern Indian Ocean. In the lower troposphere (850-hPa), anti-cyclonic anomalies were clearly observed in the central to eastern Pacific, while equatorial-symmetric cyclonic anomalies related to equatorial Rossby waves were observed in the Indian Ocean.

The above-mentioned features of convective activities and circulation in the tropics had impacts on the tropical climate, such as heavy precipitation in the Philippines, the Indochina Peninsula, Melanesia and northern Brazil. Particularly, a large-scale landslide occurred in Leyte Island, the Philippines, in February, causing more than 1000 deaths or missing, according to media reports. It is thought that this landslide was caused partly by heavy rain induced by the sustained active convection associated with this La Niña event.

On the other hand, impacts of this La Niña event on atmospheric circulation were less typical and regionally restricted in the mid- and high-latitudes. However, the extremely active convection across the Bay of Bengal to the Philippine Sea in December, which may have been caused and maintained by this La Niña event, was related to extreme cold weather in and around Japan.

(1 and 2: Ikuo Yoshikawa and 3: Hiroshi Nakamigawa, Climate Prediction Division)

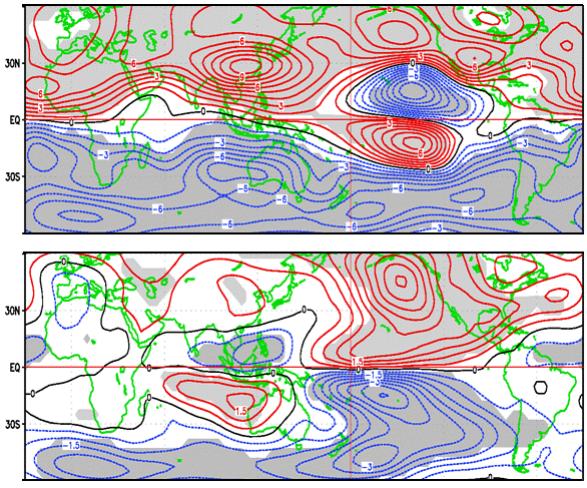

Figure 6 3-month Mean 200hPa (upper panel)/850hPa (lower panel) Stream Function regressed on an High Cloud Amount Index in the vicinity of the Indonesia (5°N-5°S,110°E-135°E) in DJF
The index shows the area-averaged high-cloud amount (the percentage of cloud cover whose top is above 400-hPa) anomalies normalized by its standard deviation in 1987-2000. Counter interval is 1×10^6 m^2/s. Shading shows 95 % confidence level based on the F-test.

Coming Soon: Climate Change Monitoring Report 2005

"Climate Change Monitoring Report 2005" will be released in upcoming September. It will say that the global mean of the surface temperatures in 2005 was the second highest since 1891. Also, maximum sea ice extent in the Arctic Ocean recorded the minimum since 1979.

JMA has issued a series of "Climate Change Monitoring Reports" annually since 1996. The Reports cover the achievements of our comprehensive activities in the field of climate ranging from observation, monitoring, analysis and projection to research and development.

The latest English issue of "Climate Change Monitoring Report 2005", which covers climatic conditions of Japan and the world for the year 2005 and recent trends of greenhouse gases concentrations and the ozone layer depletion, is scheduled to be released in September 2006 on the TCC website.

Among the wide-range subjects, the following are particularly highlighted in this 2005 issue:

- Extremely high temperatures were frequently observed in tropical areas, China and Greenland. The global mean of the surface temperatures (the average of near surface air temperature over land, and sea surface temperature) in 2005 was +0.32℃ above normal (1971-2000 average), and was the second highest since 1891 only to 1998 (Figure 7).
- In the Arctic Ocean, the sea ice extent has been below normal since May 2001. In the winter of 2005, maximum sea ice extent in the Arctic Ocean recorded the minimum since 1979 when the statistics began.
- Concentration of atmospheric carbon dioxide (CO_2) has been continuously increasing through the instrumental-observation period. The annual mean concentration of CO_2 in 2005 was larger by 2.1 to 2.5 ppm than that in 2004 at all of the three observatories in Japan.
- The ozone hole over the Antarctic in 2005 was almost the averaged-size compared with those in last 10 years.

(*Hiroko Morooka, Climate Prediction Division*)

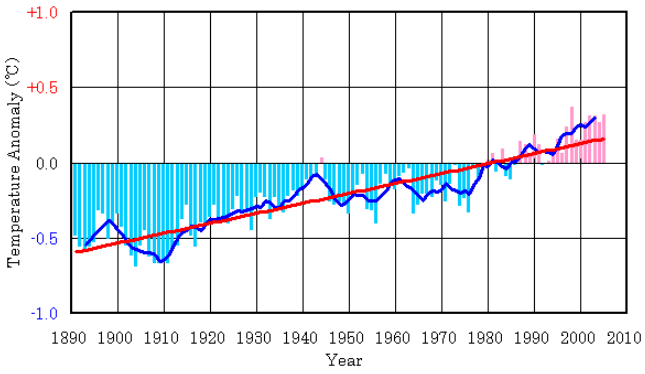

Figure 7 Annual anomalies of surface temperature (the average of near surface air temperature over land, and SST) from 1891 to 2005 over the globe
Anomalies are deviations from normal (1971-2000 average). The bars indicate anomalies of surface temperature in each year. The blue line indicates their 5-year running means, and the red line indicates the long-term linear trends.

Sea ice conditions in the Sea of Okhotsk in the 2005/2006 winter season

The accumulated sea ice extent in the Sea of Okhotsk through the winter season was the smallest since 1970/1971. Also, the maximum sea ice extent in the region was the second smallest only to 1983/1984.

Sea ice extent in the Sea of Okhotsk was much smaller than normal throughout the 2006 sea ice season (from December 2005 to May 2006). Accumulated sea ice extent, which is defined as the seasonal sum of sea ice extents at five-day intervals from December in the previous year to May and used as an index of the magnitude of sea ice extent in the sea ice season, was the smallest since 1971. Its ratio to normal (1971-2000 average)

Table 3 Ranking of the smallest five accumulated sea ice extents in the Sea of Okhotsk
Accumulated sea ice extent from December in the previous year to May in the Sea of Okhotsk has been observed since 1971. The normal is 30-year average from 1971 to 2000.

Rank	Year	Ratio to normal
1	2006	64%
2	1996	66%
3	1991	71%
4	2005	73%
5	1984	74%

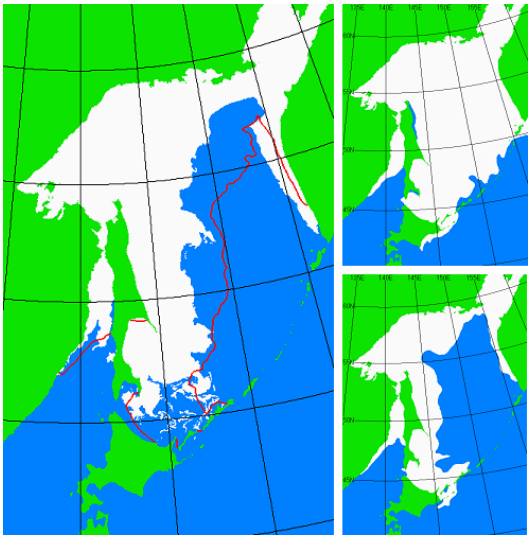

Figure 8 Seasonal maximum sea ice extents
The left panel shows the seasonal maximum sea ice extent in the 2006 sea ice season (10 March 2006). The red line indicates the edge of normal sea ice extent. The upper right panel shows the largest one (28 February 1978) and the lower right panel shows the smallest one (25 February 1984) since 1971.

was 64% (Table 3). Sea ice extent reached its seasonal maximum of 0.90 million square kilometers on 10 March 2006, which was the second smallest only to 0.86 million for the year 1984 (Figure 8). The details are shown at http://okdk.kishou.go.jp/news/topics_20060526.html.

The small sea ice extent in the 2006 sea ice season was presumably due mainly to the following two reasons (Figure 9):

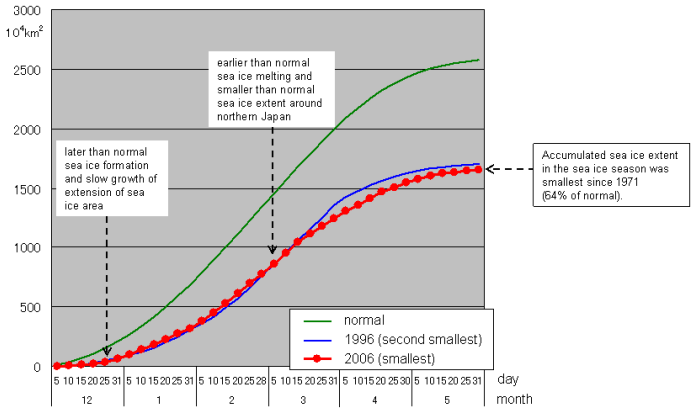

Figure 9 Progress of accumulated sea ice extent in the Sea of Okhotsk

Accumulated sea ice extent in this figure is defined as the sum of sea ice extents at five-day intervals from the beginning of the sea ice season (December in the previous year) up to each date shown along the abscissa. The red, blue and green lines indicate the progress of the accumulated sea ice extent in the 2006 season, in the 1996 season and in the normal (1971-2000 average), respectively. The accumulated sea ice extent from December to May in the 2006 season is the smallest since 1971, and the one in the 1996 season is the second smallest.

1. Air temperatures and sea surface temperatures were higher than normal in and around much of the Sea of Okhotsk in November and December 2005, which led to later than normal sea ice formation and slow growth of sea ice area.
2. Air temperatures were higher than normal around northern Japan from the middle of February to the end of March 2006, which resulted in earlier than normal sea ice melting and smaller than normal sea ice extent around northern Japan.

Although variations with decadal or near-decadal time scales are seen in the sea ice extent in the Sea of Okhotsk, no explicit long-term trend has been found (Figure 10).

(*Takafumi Umeda, Office of Marine Prediction*)

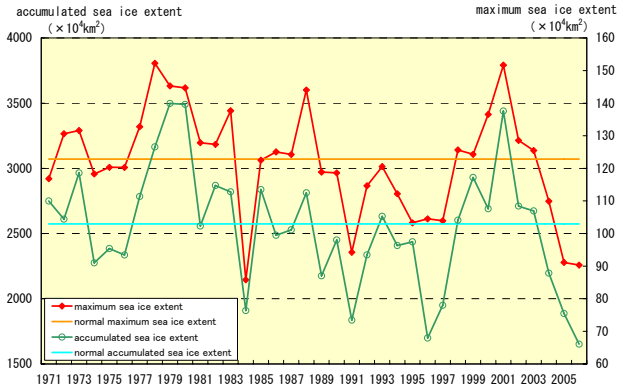

Figure 10 Inter-annual variations of seasonal maximum sea ice extent (red line; scale on right axis) and accumulated sea ice extent in the sea ice season (green line; scale on left axis) in the Sea of Okhotsk

Summary of yellow sand over Japan in 2006

The total number of days when yellow sand, Asian dust, was observed in Japan between January and May 2006 was 42, the fourth largest since 1967. For Tokyo, it was the first time for last six years that yellow sand was observed.

1. Occurrences of yellow sand over Japan in spring 2006

The total number of days of yellow sand, which is the aeolian dust transported from the Asian continent, observed in Japan was 42 during January through May 2006, which is the fourth largest since 1967. The daily number of meteorological stations which reported yellow sand notification was 446 in April 2006, which is the second largest only next to April 2002, when it was 593. Yellow sand was observed extensively over Japan three times, from 8th to 9th April, from 18th to 19th April and from 24th to 25th April. In Tokyo, yellow sand was observed from 18th to 19th April, which was the first time since 14th April 2000, and attracted public interest very much (Figure 11). The Annual course

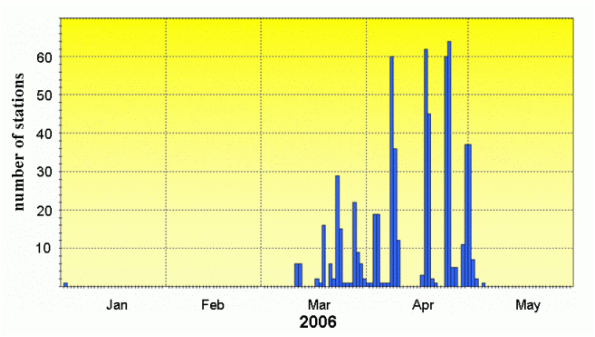

Figure 11 The daily number of meteorological stations which reported yellow sand notification (from 1 January 2006 to 31 May 2006)

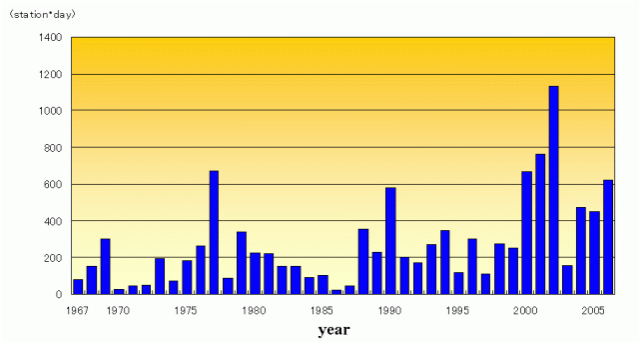

Figure 12 Annual course of the total daily number of meteorological stations which reported yellow sand notification (from 1967 to 2006)

The number for 2006 is accumulated from January to May. Statistics are based on observations of 103 observatories in Japan.

of the total daily number of meteorological stations which reported yellow sand notification shows large year-to-year fluctuation and does not exhibit any clear long-term trends, though it reached the largest number, 1132, in 2002 (Figure 12).

2. Possible factors of the frequent yellow sand occurrences over Japan

According to the monthly climate reports from China and Mongolia, the 5-month total precipitation amounts from December 2005 through April 2006 were around 40% to 70% of normal at many observatories in Mongolia and the northern part of China (Figure 13), both of which are one of the origins of yellow sand. It is inferred from satellite observations that the days of snow cover were less than normal in those areas (http://okdk.kishou.go.jp/products/clisys/m03/f601m03.html). These facts indicate that the soil moisture conditions in those areas seemed to be drier than normal. As features of the atmospheric circulation in April 2006, north-westerly upper air flow was prevailed and the high frequency disturbances were much more active than normal from western Siberia to Japan (Figure 14 and 15). Though the occurrence of yellow sand is also related to the change of vegetation and the land use, it is thought that the frequent observations of yellow sand over Japan in this spring were affected by the following factors: drier than normal soil moisture condition, the frequent occurrence of dust storms due to the active synoptic disturbances and the upper air flow direction which is favorable to bringing the blown-up sand to Japan.

(*Kohei Honda, Atmospheric Environment Division*)

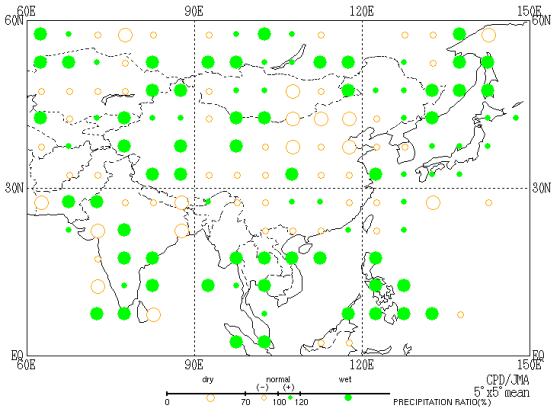

Figure 13 Precipitation ration in December 2005 – April 2006
Green and orange circles indicate 5 degree x 5 degree average of precipitation ratio.

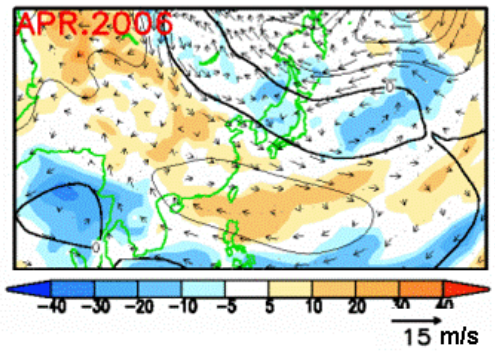

Figure 14 Monthly mean anomalies of 500hPa stream function, wind & OLR in April 2006
Contours show stream function (x$10^6$$m^2$/s). Vectors show wind vector (m/s). Shading shows OLR (W/m^2).

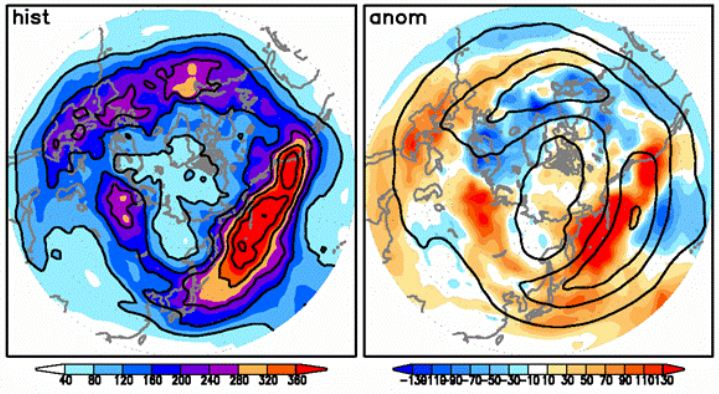

Figure 15 Kinetic energy of high-frequency variation at 500-hPa in April 2006
Left and right panels show historical and anomaly map, respectively. Kinetic energy per unit mass of high-frquency variation (unit: m^2/s^2) at 500-hPa indicates the activity of synoptic-scale disturbance. It is defined as root mean square of zonal and meridional wind speed of 2-8-day band-pass-filtered as described by Duchon (1979) based on 6-hourly analysis.

Current status of the yellow sand forecasting research

To provide yellow sand (aeolian dust) forecast and to study the impact on the climate due to dust, a global dust transport model has been developed by the Meteorological Research Institute (MRI). It is shown that dust from the Gobi and the Taklimakan desert has different transport routes, and dust may have a significant impact on the atmospheric environment and climate on the regional scale.

Yellow sand phenomenon has been frequently observed in recent years over wide area of East Asia which includes Japan. Because it often causes air pollution and gives crucial damage to the society (e.g., to public transport through the degradation of visibility and to human health through the infirmity of respiration), the yellow sand information is required. From January 2004, Japan Meteorological Agency (JMA) has been providing yellow sand information, which include observed dust weather and the operational numerical forecast of yellow sand (http://www.jma.go.jp/jp/kosa/index.html).

To make the forecast of yellow sand, JMA is operating a numerical dust model, which is coupled with a general circulation model, MRI/JMA 98 (Tanaka and Chiba, 2005) and is called the Model of Aerosol Species IN the Global Atmosphere (MASINGAR). This dust model calculates the dust emission from the surface wind shear stress, soil moisture, snow cover, and vegetation, and computes the atmospheric concentration of dust particles from advective transport, convective transport, turbulent mixing, dry deposition

and wet deposition. The model has been developed at the atmospheric environment and applied meteorology department of MRI as a part of Japan-China Joint Project Aeolian Dust Experiment on Climate impact (ADEC) (Mikami et al., 2005), and is continuously checked and improved in order to yield better model performance.

Figure 16 shows an example of a dust simulation with MASINGAR. The figure separately displays the dust originated from the Gobi and the one from the Taklimakan desert. As evidently seen in Figure 16, it has been found from a lot of simulations with MASINGAR that the dust from the Gobi desert tends to be transported at lower altitude, and affect the air quality in the densely populated areas on the downwind of the source region. On the other hand, the dust from the Taklimakan desert tends to be transported at higher altitude and to reach longer distance. It is also suggested that the dust from the Sahara desert or Arabian Peninsula may affect the East Asian environment at the background level (Tanaka et al., 2005).

Yellow sand also has an impact on the climate by scattering and/or absorbing the solar and terrestrial radiation. Figure 17 shows the annually averaged radiative perturbation at the top of the atmosphere simulated by MASINGAR. It is suggested that dust cools the areas with low albedo (oceans and densely vegetaged land), and warms the areas with high albedo (deserts, cryosphere, and regions with frequent lower clouds). The radiative perturbations over desert area could be very large (~ 10 W m^{-2}), so that the dust exerts a significant impact on the atmospheric environment and climate on a regional scale.

(*Taichu Y. Tanaka, Meteorological Research Institute*)

Acknowledgment
The author is grateful to Takashi Maki, Kiyotaka Shibata, and Masao Mikami for reviewing the manuscript.

References

Mikami, M., et al., 2006: Aeolian Dust Experiment on Climate Impact: An Overview of Japan-China Joint Project ADEC, *Global Planetary Change* **52**, 142–172.

Tanaka, T. Y., Chiba, M., 2005: Global simulation of dust aerosol with a chemical transport model, MASINGAR. *J. Meteor. Soc. Japan* **83A**, 255–278.

Tanaka, T. Y., et al., 2005: Possible transcontinental dust transport from North Africa and the Middle East to East

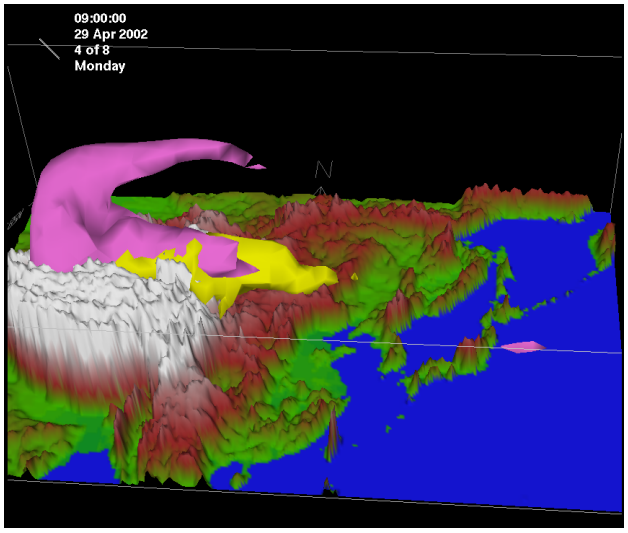

Figure 16 A 3-dimensional image of East Asian dust on 25 April, 2002 simulated with MASINGAR
The yellow color displays the dust from eastern China (the Gobi desert), and the pink color denotes the dust from western China (the Taklimakan desert).

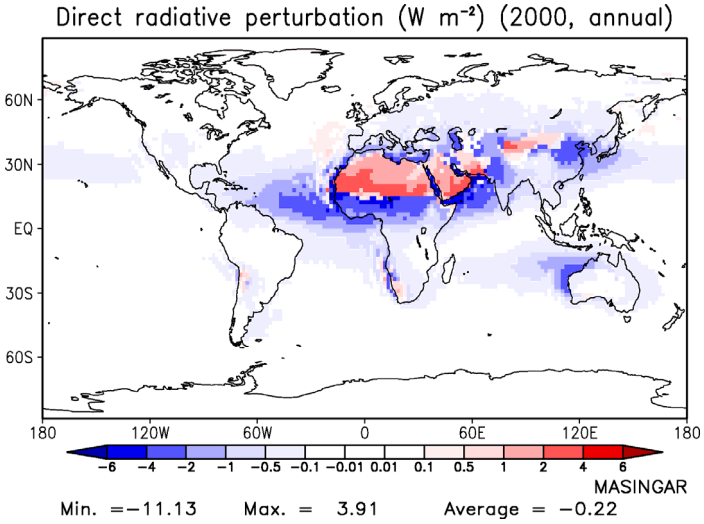

Figure 17 Simulated annual mean distribution of the radiative perturbation of dust at the top of the atmosphere
The blue shading indicates cooling, and the red shading indicates warming of the atmosphere and the Earth. The unit is W m^{-2}.

Opening of the new website for providing the JRA-25 official data

The JRA-25 official data was released on 18th July 2006. The JRA-25 reanalysis data, which gives 6-hourly atmospheric fields for 26 years from 1979 to 2004, was produced by JMA (Japan Meteorological Agency) and CRIEPI (Central Research Institute of Electric Power Industry). The data is available via the Internet for any research use. Please visit the JRA-25 official page (http://jra.kishou.go.jp/) and take necessary procedure according to the guidance there.

Any comments or inquiries on this newsletter and/or the TCC website would be much appreciated. Please e-mail to the following address:
tcc@climar.kishou.go.jp
(Chief Editor: Shingo Yamada)

Tokyo Climate Center (TCC), Climate Prediction Division, JMA
Address: 1-3-4 Otemachi, Chiyoda-ku, Tokyo 100-8122, Japan
TCC website: http://okdk.kishou.go.jp/index.html